

A Novel Reduced Graphene Oxide/ β -Cyclodextrin/Tyrosinase Biosensor for Dopamine Detection

Luminița Fritea^{#1,2}, Mihaela Terțiș^{#1}, Serge Cosnier², Cecilia Cristea^{1,*}, Robert Săndulescu¹

¹Analytical Chemistry Dept, Faculty of Pharmacy, "Iuliu Hațieganu" University of Medicine and Pharmacy, 4 Pasteur Street, 400349, Cluj-Napoca, Romania

²Univ. Grenoble Alpes, DCM UMR 5250, F-38000 Grenoble, France; CNRS, DCM UMR 5250, F-38000 Grenoble, France

*E-mail: ccristea@umfcluj.ro

#Authors with equal contribution

Received: 29 May 2015 / Accepted: 30 June 2015 / Published: 28 July 2015

A graphene/ β -cyclodextrin biosensor with tyrosinase was developed by combining the enhanced sensitivity given by the special properties of graphene and cyclodextrin, and the specificity of the enzyme for dopamine detection. The nanoplatform was achieved by layer-by-layer deposition and various parameters were optimized by using square wave voltammetry. Microscopic and spectral techniques (Raman, FTIR) were used to characterize the modification of graphene oxide and of the glassy carbon electrodes. The biosensor was successfully applied for dopamine determination in pharmaceutical products, human serum and urine with good recoveries, by using amperometry.

Keywords: reduced graphene oxide, β -cyclodextrin, tyrosinase, pharmaceutical and biological analysis

1. INTRODUCTION

Dopamine (DA) is a neurotransmitter which is implicated in several nervous system disorders such as schizophrenia, Parkinson's disease and Huntington's disease. The real-time detection of low DA levels being of particular importance, many research studies were conducted towards the elaboration of electrochemical sensors ensuring its fast and sensitive detection. Several other biological molecules, such as glucose, ascorbic and uric acids, etc., usually found in real complex matrixes, generate interferences, affecting thus the accurate determination of DA [1, 2].

Many types of modifiers including Nafion and other polymers, carbon nanotubes and metallic nanoparticles, self-assembled monolayers or organic redox mediators were used to modify the

electrodes for dopamine detection [2-10]. Recently, graphene, a two-dimensional carbon-based nanomaterial and its reduced form, reduced graphene oxide (RGO), have attracted considerable interest. Their electrocatalytic activity, their wide potential window, and other impressive electronic properties have promoted their broad use in electrochemical sensing and biosensing applications [11-14]. Moreover, its association with cyclodextrins (CDs) was also reported for the DA detection. These cyclic oligosaccharides consisting of 7, 8 and 9 glucopyranose units possess a torus hydrophobic cavity, which can interact with various organic and inorganic molecules leading to host-guest complexes. Different biological substances were determined with high sensitivity and selectivity by using their complexation ability [15-17]. Recently, the electrodes modified with graphene and cyclodextrins have been widely employed for the DA detection, alone or with various interfering analytes [1, 18-26].

The elaboration of a nanostructured electrode material obtained by layer-by-layer (LBL) association of RGO, β -cyclodextrin (β -CD) and polyethylenimine (PEI) is reported. The conducting polymer was used for the immobilization of the tyrosinase (TYR), which catalyzes the oxidation of phenolic compounds such as DA into quinone derivatives. This enzyme electrode allows the amperometric DA detection via the reduction of the enzymatically generated quinone avoiding thus the interference with different easily oxidizable endogenous species such as ascorbic acid and uric acid.

A glassy carbon electrode (GCE) was modified with graphene oxide reduced with ascorbic acid, a simple method which avoids the environmentally harmful reducing agents [27], β -CD and (PEI) by using LBL method. The obtained nanocomposite material was then characterized and optimized for the electrochemical detection of DA. After TYR immobilization, the resulting biosensor was used for the detection of DA in pharmaceutical products and biological fluids in the presence of some possible interfering species.

2. EXPERIMENTAL

2.1. Reagents and solutions

β -CD was purchased from Merck and graphene oxide (GO), TYR, normal human serum and dopamine hydrochloride from Sigma Aldrich. Phosphate buffer solutions (PBS) were prepared with sodium dihydrogen phosphate, sodium monohydrogen phosphate from Sigma (pH 7.2; 0.1M). Ultrapure water (Milli Q Barnstead EASY pure Rodi) was used for the preparation of all aqueous solutions and the experiments were done at 25°C.

The RGO modified with β -CD (RGO- β -CD) was prepared as follows: 30 mg GO were dispersed in 60 ml water and were sonicated for 2 hours, 60 mL of β -CD solution (4 mg/mL) were then added and stirred together for 30 minutes. Then 600 mg of ascorbic acid were dissolved and the final suspension was stirred for 48 hours. The preparation of the unmodified RGO was similar to the procedure mentioned above without the addition of β -CD [27, 28].

The suspension was centrifugated and the ascorbic acid was removed by washing with plenty of ultrapure water. The RGO powder was dried in oven and suspended in water (1 mg/mL). The suspension was sonicated for 1 hour before its use for the electrode modification. Ultrapure water was

used for the preparation of 1 mg/mL β -CD and 1 mg/mL TYR solutions, while 1 mg/mL PEI solution was prepared in water:ethanol (1:1) mixture.

2.2. Biosensor preparation

GCEs, 3 mm in diameter, were purchased from BAS Inc. (Lafayette, USA), polished with diamond paste (2 μ m) and then rinsed successively with ultrapure water and ethylic alcohol. The electrode modification was carried out by LBL deposition of the different modifiers. Thus, two successive layers of 5 μ L of RGO (1 mg/mL), 5 μ L of β -CD (1 mg/mL), each of them followed by solvent evaporation in the oven at 40 °C for 10-15 minutes, were dropped onto the electrode surface (RGO/ β -CD). After that, 5 μ L of TYR (1 mg/mL) and 5 μ L of PEI (1 mg/mL) were dropped and dried at room temperature. Different configurations of bioelectrode materials were elaborated by varying the numbers of RGO and TYR layers (each layer contained 5 μ L).

2.3. Electrochemical, spectral and microscopic analysis

Electrochemical experiments were performed with an Autolab PGSTAT100 potentiostat (Metrohm/Eco Chemie Netherlands) equipped with Nova 1.10.4 software using an electrochemical cell with three electrodes: a glassy carbon working electrode, an Ag/AgCl reference electrode and a counter electrode of platinum. In the case of square wave voltammetry (SWV) experiments, the established parameters are: initial potential -0.3 V, end potential 1 V, amplitude 25 mV and a frequency of 25 Hz. The amperometric determinations were made at -0.2 V in solution kept under stirring (200 rpm).

An Alpha 300R (WiTec) confocal Raman microscope was used for the Raman spectroscopy determinations performed on the modified electrodes at 532 nm for laser and 60 seconds time accumulation, while the WiTec Control software was used for data analysis. The microscopic images were obtained with the same microscope. An Jasco FT/IR-4100 spectrophotometer controlled by an appropriate software was used for recording the FTIR spectra of the GO and RGO in the range from 550 to 4000 cm^{-1} .

2.4. Real samples preparation

The solution from 10 vials of solution for injection of DA hydrochloride 0.5 % (Zentiva, Romania) was well homogenized, after that 0.1 M PBS solution with pH 7.2 was added in order to obtain a mother solution containing 10^{-2} M DA hydrochloride. This solution was freshly prepared every day and kept in the dark place, at 4 °C to avoid DA oxidation. The DA hydrochloride was quantified from the pharmaceutical samples, using the calibration curve obtained with standard DA hydrochloride substance.

The urine was provided by a volunteer. Before analysis, the samples were filtered (paper filter FILTRAK 390) and diluted 1:100 with buffer (PBS 0.1 M, pH 7.2). The human serum was prepared as

follows: the lyophilized powder was dissolved in 2 ml of distilled water resulting 60 mg/mL of proteins and then diluted 1:100 with buffer (PBS 0.1 M, pH 7.2).

3. RESULTS AND DISCUSSION

3.1. Spectral and microscopic characterization: RAMAN, FTIR and microscopic images

In accordance with recent scientific papers [29], the characteristic Raman spectra of GO present three important bands: a strong band at 1353 cm^{-1} named D band, another strong band at 1598 cm^{-1} named G band and a weaker band named 2D band situated in the region from 2500 to 3000 cm^{-1} (Figure 1A). The pronounced diminution of the intensity for these three characteristic bands is probably due to the reduction of oxygen containing groups from GO sheets and to the partial restoration of the sp^2 graphene structure after the reduction reaction [25, 30].

In the FTIR spectra obtained in the case of GO there are present some characteristic bands that can be attributed to various functional groups such as: $\nu(\text{C-O})$ from carbonyl at 1001 cm^{-1} ; $\nu(\text{C-O})$ from carbonyl, carboxyl, ethers or alcohols at 1174 cm^{-1} ; $\nu(\text{C-C})$ from aromatics at 1507 cm^{-1} ; $\nu(\text{C=C})$ from aromatics at 1656 cm^{-1} and $\nu(\text{C=O})$ from carboxyl at 1750 cm^{-1} . This behavior was also observed and reported in other papers [29, 31-33]. In the RGO FTIR spectrum two bands from 2908 cm^{-1} and 2990 cm^{-1} $\nu(\text{C-H})$ present weaker intensities due to the disappearance of C-H bonds during the aromatization of the graphene core. The partial elimination of the oxygen from the GO structure after the reduction process can be demonstrated by the FTIR spectra obtained in the case of RGO by the decreasing of the characteristic bands in the region from 3500 to 3900 cm^{-1}) [34, 35]. The successful reduction of the GO sheets was revealed from the FTIR spectra of RGO and RGO- β -CD by summing the overall registered modifications (Figure 1B).

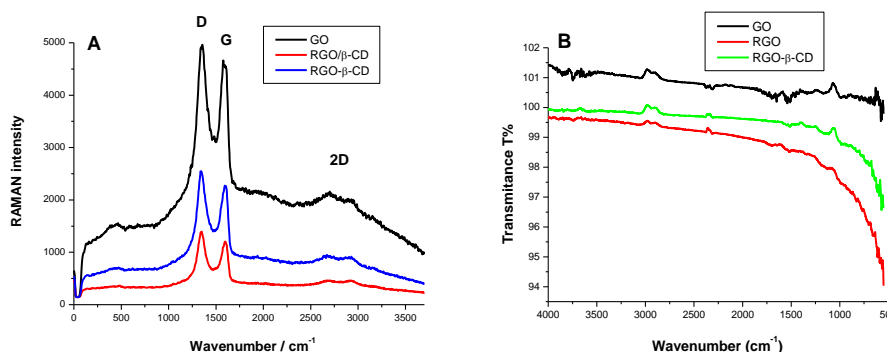


Figure 1. Raman (A) registered for: GO (black), RGO/ β -CD (red), RGO- β -CD (blue) and FTIR spectra (B) registered for: GO (black), RGO (red), RGO- β -CD (green)

The electrodes modified with thin films of GO, RGO/ β -CD and RGO- β -CD on PEDOT were characterized with a confocal Raman microscope (Figure 2). The two types of the electrodes modified

with RGO presented different characteristics because of the nanocomposite presence, revealed in the corresponding microscopic images. For the RGO modified electrode, the graphene structure was more distinguishable covering the electrode surface (Figure 2 B). For the RGO- β -CD modified electrode, the graphene sheets were more homogeneously distributed over the electrode surface (Figure 2 C).

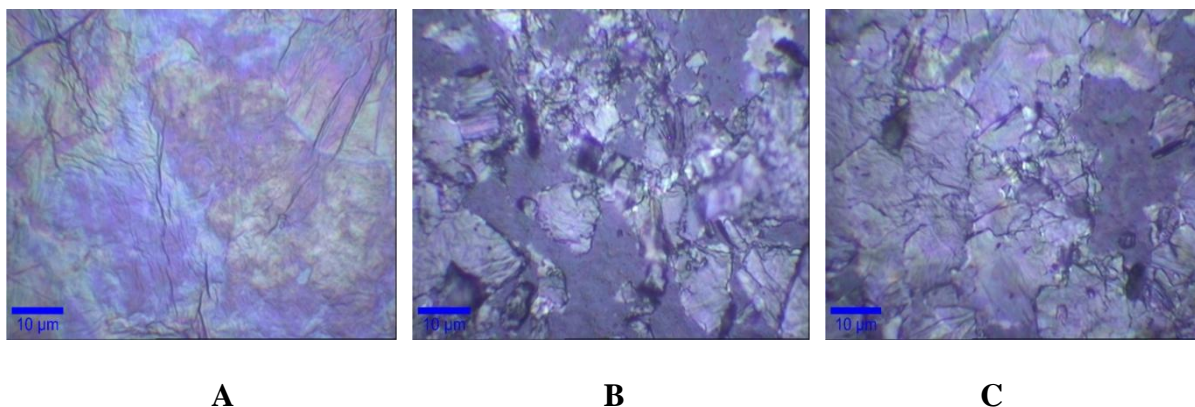


Figure 2. Microscopic images for: (A) GO/PEDOT, (B) RGO/ β -CD/PEDOT and (C) RGO- β -CD/PEDOT

3.2. Electrochemical characterization of the nanostructured electrode material

The DA response recorded by SWV was investigated on different GCEs modified with: RGO, RGO modified with β -CD (RGO- β -CD) and RGO covered with a β -CD layer (RGO/ β -CD). The best sensitivity to DA electro-oxidation was recorded with the configuration consisting in single layers of RGO, β -CD and PEI (RGO/ β -CD/PEI), respectively (Figure 3A). Comparing the DA oxidation peak intensity obtained on RGO/GCE and on RGO- β -CD/GCE, it can be observed that the oxidation potential is slightly shifted towards cathodic values due to the cavity of β -CD which facilitates the dopamine oxidation and the peak area is smaller because the graphene proportion is smaller in the RGO- β -CD nanocomposite [25].

Table 1. SWV data for the GCE modified with different numbers of RGO layers

Electrochemical parameters	RGO layers number			
	0	1	3	5
Oxidation potential (mV)	213	195	219	241
Peak intensity (μ A)	92.37	508.19	174.10	87.58
Peak surface (μ C)	25.35	95.14	22.74	10.02

The effect of RGO layers deposited on the GCE on the DA oxidation current intensity was also examined. It appears that the increasing number of RGO layers decreased the oxidation peak's intensity and surface, and slightly shifted the potential towards more anodic values (Table 1). This behavior may be due to a possible compaction of the graphene structure with the increasing deposited amount of graphene, slowing thus the electron transfer process. The most sensitive configuration for the direct determination without any preconcentration time is based on single layer of RGO (Figure 3B).

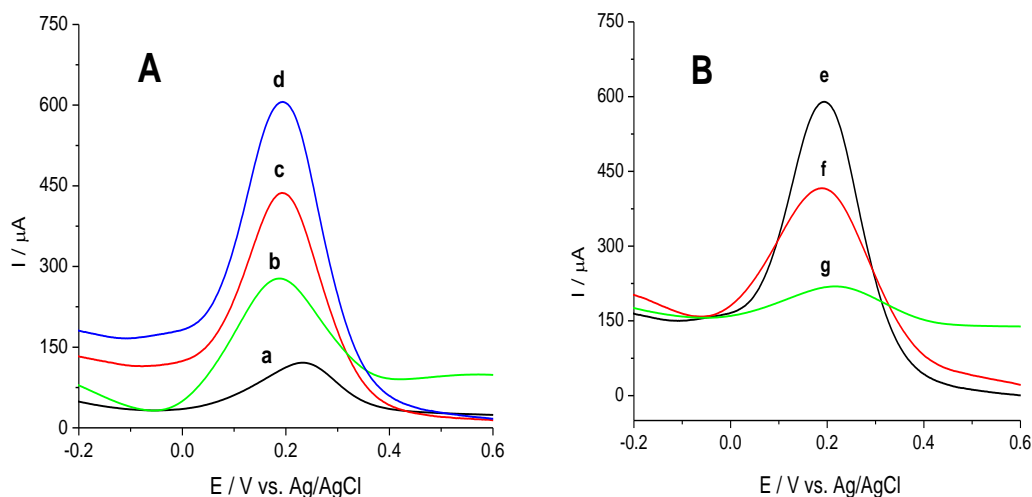


Figure 3. (A) SWVs of 10^{-3} M DA solution obtained at: (a) bare GCE; (b) GCE modified with single layers of RGO- β -CD composite and PEI; (c) GCE modified with single layers of RGO and PEI; (d) GCE modified with successive single layers of RGO, β -CD and PEI; (B) SWVs obtained for 10^{-3} M DA solution at GCE modified with a single layer of RGO after (e) 0 min, (f) 1 min and (g) 5 min of preconcentration

3.3. Electrochemical performance of the biosensor

The biosensor was assembled by depositing successive layers of RGO, β -CD and TYR entrapped in polymeric film (RGO/ β -CD/TYR/PEI), (Figure 4).

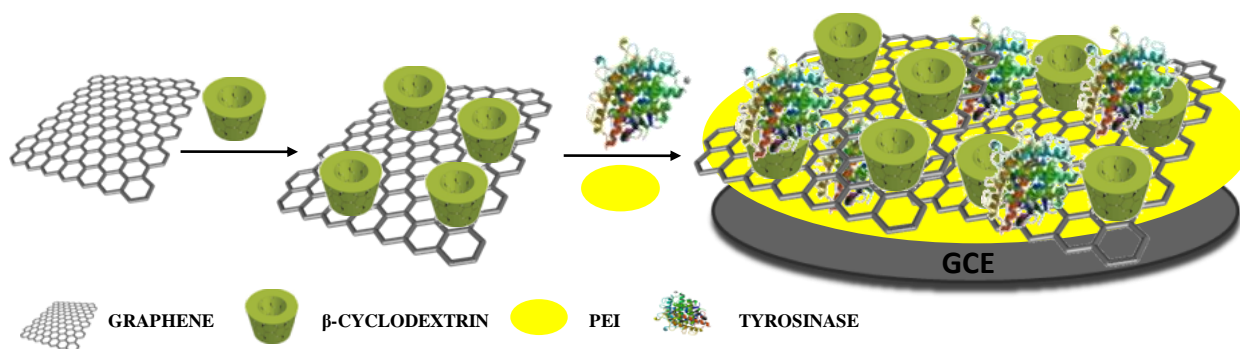


Figure 4. Schematic representation of the biosensor elaboration

Taking into account that the enzyme quantity which is immobilized at the electrode surface could modulate the biosensor performance, different amounts of TYR (15, 25 and 50 μg) were tested, the optimum configuration being obtained for 50 μg TYR. It should be noted that the enzyme is covered by a PEI film in order to avoid its loss during the amperometric analysis carried out under stirring. In addition, hydrophobic residues of appropriate size of the TYR shell can lead to host-guest interactions with the β -CD groups reinforcing its adsorption onto the graphene layer.

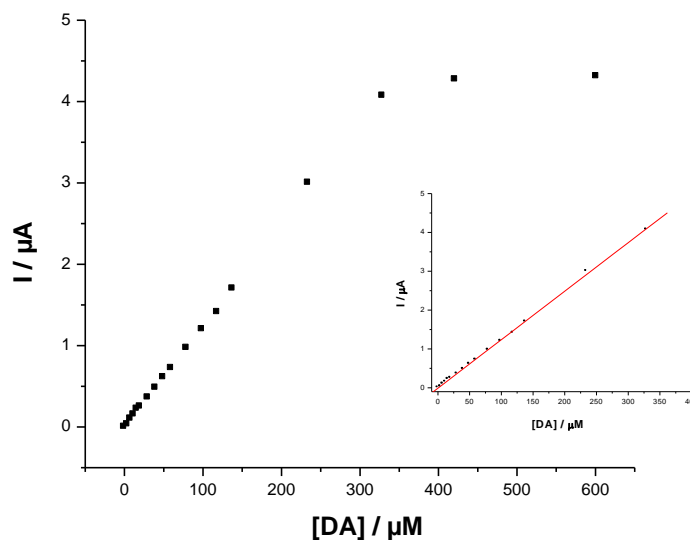


Figure 5. Calibration curve for DA recorded on RGO/ β -CD/TYR/PEI electrode (-0.2V vs Ag/AgCl in 0.1 M PBS, pH 7.2 under stirring, air-saturated solution). Inset: linear variation of the current intensity with DA concentration.

The performance of the elaborated biosensor for DA detection from pharmaceutical product and biological samples was examined by potentiostating the modified electrode at -0.2 V. Figure 5 shows the resulting calibration curve exhibiting a linear part ranging from 3.9 to 328.8 μM (I (μA) = $0.0121 \cdot C_{\text{DA}}$ (μM); $R^2 = 0.999$), with a LOD of 3.9 μM and a sensitivity of 12.1 nA/ μM . In the absence of β -CD, the LOD is markedly increased, namely 12.74 μM , highlighting the sensitivity improvement conferred by the presence of the β -CD.

3.4. Analytical performance of the biosensor in real samples

The optimized biosensor was tested for the amperometric detection of DA hydrochloride[®] 0.5% (Zentiva) at -0.2 V. The obtained results are in accordance with the Roumanian Pharmacopea [36] and the recoveries were between 96.9 % and 100.7 % (RSD ± 1.65 %).

The potential interferences with the excipients in the same concentration as in the commercial product were also evaluated. Propylene glycol 25 % and ethanol 25 % did not show any interference

with the DA signal, meanwhile 0.01 % sodium metabisulphite decreased the DA electrochemical response with 2.2 %.

The urine and human serum samples, prepared by 100 times dilution before testing, were spiked with different volumes of 10^{-2} M standard DA solution and the amperometric measurements revealed good recovery rates (Table 2).

Table 2. DA amperometric detection from urine and serum

Sample	Added DA (μM)	Peak intensity (μA)	Recovery (%)	RSD (%)
PBS	10	0.52	-	-
	20	1.10		
Urine	10	0.52	100.19	1.46
	20	1.07	97.27	
Serum	10	0.53	101.92	1.87
	20	1.08	98.18	

No significant interferences were observed, when DA was simultaneously determined by using amperometry, with equal and 10 times higher concentrations of glucose and with equal concentration of uric acid and ascorbic acid (Figure 6).

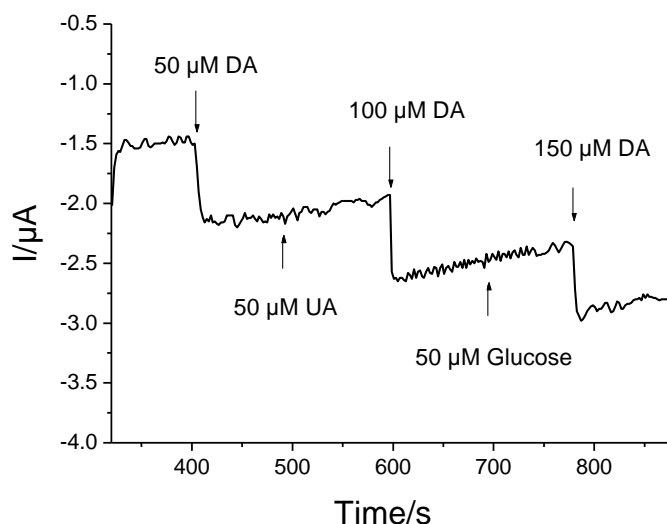


Figure 6. Amperometric current response of RGO/ β -CD/TYR/PEI electrode to successive injections of equal volumes (25 μL) of 10^{-2} M of DA, UA and glucose solutions in PBS, each step corresponding to 50 μM . Experimental conditions as in Figure 5.

The analytical results obtained by using the elaborated biosensor were compared with others electrochemical sensors performances which are presented in Table 3.

Table 3. Electroanalytical performances of some graphene based sensors for DA detection

Electrode configuration	Detection method	LOD (μM)	Linear range (μM)	Simultaneously tested compounds	References
GO/GCE ¹	DPV	0.27	1-15	AA, UA	[1]
ERGO/GCE ²	DPV	0.5	0.5-60	AA, UA	[18]
RGO/GCE ³	DPV	2.64	4-100	AA	[19]
TCPP/CCG/GCE ⁴	DPV	0.01	0.01-70	AA, UA	[20]
RGO/CS/GCE ⁵	DPV	-	5-200	AA, UA	[21]
Graphene/Ppy/GCE ⁶	CV	0.1	25-1000	AA	[22]
RGO/AuNP/ GCE ⁷	DPV	0.6	0.6-44	UA	[23]
GS/poly-CD/MWCNTs/GCE ⁸	CV	0.05	0.15-22	AA, NO ₂ ⁻	[24]
RGO/ β -CD/GCE ⁹	CV, Amperometry	0.005	0.9-200	AA	[25]
AuNP/ β -CD/RGO ¹⁰	SWV	0.15	0.5-150	AA, UA	[26]
RGO/ β -CD/TYR/PEI/GCE ¹¹	Amperometry	3.9	3.9-329	AA, UA, glucose	This work

DPV = differential pulse voltammetry; CV = cyclic voltammetry; SWV = square wave voltammetry
AA = ascorbic acid; UA = uric acid

¹GO/GCE = glassy carbon electrode modified with covalently attached graphene oxide via NHS/EDC chemistry

²ERGO/GCE = GCE modified with electrochemically reduced GO (at the electrode surface)

³RGO/GCE = GCE modified with chemically reduced GO (in suspension)

⁴TCPP/CCG/GCE = GCE modified with meso-tetra (4-carboxyphenyl)porphine and chemically reduced graphene

⁵RGO/CS/GCE = GCE modified with chemically reduced GO entrapped in chitosan film

⁶Graphene/Ppy/GCE = GCE modified with graphene entrapped in overoxidized polypyrrole

⁷RGO/AuNP/ GCE = GCE modified with electrochemically reduced GO and electrochemically generated gold nanoparticles

⁸GS/poly-CD/MWCNTs/GCE = GCE modified with graphene sheets, poly-cyclodextrin polymer and multiwall carbon nanotubes

⁹RGO/ β -CD/GCE = GCE modified with chemically reduced GO and β -CD

¹⁰AuNP/ β -CD/RGO = GCE modified with AuNPs, β -CD and thermal reduced GO

¹¹RGO/ β -CD/TYR/PEI/GCE = GCE modified with chemically reduced GO, β -CD and tyrosinase entrapped in polyethylenimine polymer.

It can be observed that this biosensor can be applied for DA determination on a wider linear range than most of the above mentioned sensors. It is noteworthy to mention that the LOD was experimentally determined proving clearly that this biosensor is able to detect 3.9 μM of DA, whereas in the majority of the cases reporting lower LOD it was calculated. The tyrosinase presence improves the specificity and selectivity of the biosensor allowing thus the accurate DA detection in real samples without complex samples pretreatment and in the presence of common interfering species. Other properties of this electrochemical biosensor such as less time-consuming and less cost-effective make it suitable for fast and sensitive DA determination.

4. CONCLUSIONS

This work shows the new possibilities open by the efficient layer-by-layer deposition of reduced graphene oxide, β -cyclodextrin, enzyme and polyethyleneimine for the elaboration of

biosensor. Such procedure applied to the immobilization of tyrosinase thus allowed the dopamine determination with high sensitivity and selectivity. The biosensor configuration was optimized in terms of layers number, type of graphene, accumulation time and deposition method. The applicability of this newly designed amperometric biosensor for dopamine detection in pharmaceutical products and biological fluids (serum samples and urine samples) has been demonstrated.

ACKNOWLEDGEMENTS

Special thanks to Cosmin Farcău, PhD, Prof. Iuliu Marian, PhD, Tamara Liana Topală, PhD for spectral analysis and to Karine Gorgy, PhD and Alan Le Goff, PhD for their kind revision. This paper was published under the frame of European Social Found, Human Resources Development Operational Programme 2007-2013, project no. POSDRU/159/1.5/S/136893. This paper was published under the frame of European Social Found, Human Resources Development Operational Programme 2007-2013, project no. POSDRU/159/1.5/S/138776. This work was financially supported by UEFISCDI, through the project number PN-II-ID-PCE-2011-3-0355.

References

1. F. Gao, X. Cai, X. Wang, C. Gao, S. Liu, F. Gao, Q. Wang, *Sensor. Actuat. B-Chem.*, 186 (2013) 380
2. A. Gaied, N. Jaballah, M. Tounsi, M. Braiek, N. Jaffrezic-Renault, M. Majdoub, *Electroanal.*, 26 (2014) 1
3. V.T. Huong, T. Shimanouchi, D.P. Quan, H. Umakoshi, P.H. Viet, R. Kuboi, *J. Appl. Electrochem.*, 39 (2009) 2035
4. S.R. Ali, Y. Ma, R.R. Parajuli, Y. Balogun, W.Y. Lai, H. He, *Anal. Chem.*, 79 (2007) 2583
5. J. Chen, J. Zhang, X. Lin, H. Wan, S. Zhang, *Electroanal.*, 19 (2007) 612
6. R.K. Shervedani, M. Bagherzadeh, S.A. Mozaffari, *Sensor. Actuat. B-Chem.*, 115 (2006) 614
7. S. Thiagarajan, S-M. Chen, *Talanta*, 74 (2007) 212
8. T.H. Tsai, Y.C. Huang, S-M. Chen, M.A. Ali, F.M.A. Al Hemaïd, *Int. J. Electrochem. Sci.*, 6 (2011) 6456
9. Y. Zhang, Y. Pan, S. Su, L. Zhang, S. Li, M. Shao, *Electroanal.*, 19 (2007) 1695
10. M-R. Bujduveanu, W. Yao, A. Le Goff, K. Gorgy, D. Shan, G-W. Diao, E-M. Ungureanu, S. Cosnier, *Electroanal.*, 25 (2013) 613
11. S. Kochmann, T. Hirsch, O.S. Wolfbeis, *TrAC-Trends Anal. Chem.*, 39 (2012) 87
12. M. Pumera, A. Ambrosi, A. Bonanni, E.L.K. Chng, H.L. Poh, *TrAC Trends Anal. Chem.*, 29 (2010) 954
13. Z. Sun, J. Vivekananthan, D.A. Guschin, X. Huang, V. Kuznetsov, P. Ebbinghaus, A. Sarfraz, M. Muhler, W. Schuhmann, *Chem. Eur. J.*, 20 (2014) 5752
14. M. Singh, M. Holzinger, M. Tabrizian, S. Winters, N.C. Berner, S. Cosnier, G.S. Duesberg, *J. Am. Chem. Soc.*, 137 (2015) 2800
15. L. Fritea, M. Tertis, C. Cristea, R. Săndulescu, *Sensors*, 13 (2013) 16312
16. L. Fritea, M. Tertis, C. Cristea, S. Cosnier, R. Săndulescu, *Anal. Lett.*, 48 (2015) 89
17. M. Holzinger, M. Singh, S. Cosnier, *Langmuir*, 28 (2012) 12569
18. L. Yang, D. Liu, J. Huang, T. You, *Sensor. Actuat. B-Chem.*, 193 (2014) 166
19. Y-R. Kim, S. Bong, Y-J. Kang, Y. Yang, R.K. Mahajan, J.S. Kim, H. Kim, *Biosens. Bioelectron.*, 25 (2010) 2366
20. L. Wu, L. Feng, J. Ren, X. Qu, *Biosens. Bioelectron.*, 34 (2012) 57
21. Y. Wang, Y. Li, L. Tang, J. Lu, J. Li, *Electrochem. Commun.*, 11 (2009) 889

22. Z. Zhuang, J. Li, R. Xu, D. Xiao, *Int. J. Electrochem. Sci.*, 6 (2011) 2149
23. J. Du, R. Yue, F. Ren, Z. Yao, F. Jiang, P. Yang, Y. Du, *Gold Bull.*, 46 (2013) 137
24. Y. Zhang, R. Yuan, Y. Chai, W. Li, X. Zhong, H. Zhong, *Biosens. Bioelectron.*, 26 (2011) 3977
25. L. Tan, K-G. Zhou, Y-H. Zhang, H-X. Wang, X-D. Wang, Y-F. Guo, H-L. Zhang, *Electrochem. Commun.*, 12 (2010) 557
26. X. Tian, C. Cheng, H. Yuan, J. Du, D. Xiao, S. Xie, M.M.F. Choi, *Talanta*, 93 (2012) 79
27. D. Lu, S. Lin, L. Wang, X. Shi, C. Wang, Y. Zhang, *Electrochim. Acta*, 85 (2012) 131
28. Y. Guo, S. Guo, J. Li, E. Wang, S. Dong, *Talanta*, 84 (2011) 60
29. K. Bustos-Ramírez, A. L. Martínez-Hernández, G. Martínez-Barrera, M. de Icaza, V. M. Castaño, C. Velasco-Santos, *Materials*, 6 (2013) 911
30. X. Hu, R. Qi, J. Zhu, J. Lu, Y. Luo, J. Jin, P. Jiang, *J. Appl. Polym. Sci.*, 131 (2014) DOI: 10.1002/APP.39754
31. C. Shan, H. Yang, D. Han, Q. Zhang, A. Ivaska, L. Niu, *Langmuir*, 25 (2009) 12030
32. C. Shan, H. Yang, J. Song, D. Han, A. Ivaska, L. Niu, *Anal. Chem.*, 81 (2009) 2378
33. S. Stankovich, R. D. Piner, X. Chen, N. Wu, S. B. T. Nguyen, R. S. Ruoff, *J. Mater. Chem.*, 16 (2006) 155
34. S. Pei, H-M. Cheng, *Carbon*, 50 (2012) 3210
35. E-Y. Choi, T. H. Han, J. Hong, J. E. Kim, S. H. Lee, H. W. Kim and S. O. Kim, *J. Mater. Chem.*, 20 (2010) 1907
36. *Farmacopeea Română*, 10th ed., Editura Medicală: Bucharest, Romania (2008)

© 2015 The Authors. Published by ESG (www.electrochemsci.org). This article is an open access article distributed under the terms and conditions of the Creative Commons Attribution license (<http://creativecommons.org/licenses/by/4.0/>).